Carboxymethylation of Cinnamyl Alcohol with Dimethyl Carbonate over Graphitic Carbon Nitrides

Shcherban, Nataliya D.; Kholkina, Ekaterina; Sergiienko, Sergii; Kovalevsky, Andrei V.; Bezverkhyy, Igor; Murzin, Dmitry Yu

Published in:
ChemPlusChem

DOI:
10.1002/cplu.202300600

E-pub ahead of print: 23/11/2023

Document Version
Final published version

Document License
CC BY

ChemPlusChem

Research Article
doi.org/10.1002/cplu.202300600

Chemistry Europe
European Chemical Societies Publishing

www.chempluschem.org

Special Collection

Carboxymethylation of Cinnamyl Alcohol with Dimethyl Carbonate over Graphitic Carbon Nitrides

Nataliya D. Shcherban,*[a, b] Ekaterina Kholkina,[b] Sergii Sergiienko,[c] Andrei V. Kovalevsky,[d] Igor Bezverkhyy,[e] and Dmitry Yu. Murzin*[b]

A set of graphitic carbon nitride samples was prepared using a straightforward experimental procedure without templates and any subsequent treatments. The materials were studied in-depth using a range of physical and chemical methods such as X-ray diffraction, FTIR spectroscopy, elemental analysis (CHN), nitrogen physisorption, SEM, XPS, TPD CO_2. The resulting g-C_3N_4 was shown to be highly efficient in carboxymethylation of cinnamyl alcohol with dimethyl carbonate yielding up to ca. 82% of the desired cinnamyl methyl carbonate. In the studied conditions, an increase in the surface N atomic content leads to an increase in selectivity towards the desired carbonate, while a higher surface O content was beneficial for side products. Metal-free graphitic carbon nitride was shown to be one of the most productive (ca. 2 mol/h kg_{cat}) in the investigated reaction among studied heterogeneous catalysts.

Introduction

Carbonate esters not only serve as important building blocks in organic synthesis[1] capable to undergo, for instance, asymmetric allylic alkylation[2] and substitution,[3] allylic arylation,[4] the Tsuji-Trost allylation,[5] but also as protecting agents of alcohols and phenols owing to their high stability, especially in basic media.[6,7] In addition, carbonate esters arouse interest as green solvents, fuel additives as well as lubricating oils.[8,9]

Environmentally-unfriendly homogeneous catalysts such as phosgene, trimethylamine, pyridine, etc. initially applied for synthesis of carbonate esters, additionally suffer from non-reusability and a necessity of complicated separation from the reaction products.[10] An alternative chemical route includes a green carboxymethylation reagent – dimethyl carbonate (DMC) – and effective heterogeneous catalysts.[11] It worth noting that nontoxic dimethyl carbonate being both a solvent and a versatile reagent prepared from a greenhouse gas – carbon dioxide – can be successfully applied per se for upgrading of the biobased platform chemicals. Such upgrading includes methylation and methoxycarbonylation. Moreover, DMC can be used for the production of polymers or as a solvent for the metathesis reaction and Michael condensation.[12–15]

Preparation of carbonate esters from DMC and corresponding alcohols (Scheme 1) was reported using various solid base and acid catalysts[11,16–22] along with the homogeneous ones.[23] Heterogeneous catalysts are considered to be more preferable providing a more sustainable technology. In particular, commercially available basic catalysts including inorganic salts K_2CO_3, CsF/αAl_2O_3, zeolites NaX and NaY, as well as an ionic liquid $[P_{8881}][CH_3OCOO]$ were reported to be efficient (conversion > 90%, selectivity > 80%) in the methylation and transesterification of cinnamyl alcohol and 4-(3-hydroxypropyl)phenol chosen due to the resemblance with p-coumaryl alcohol reflecting the lignin structure.[16] Sodium aluminate prepared via a spray drying method was active for carboxymethylation of various alcohols resulting in unsymmetrical carbonate esters (alcohol conversion of 97% after 24 h).[11] Impregnation of $NaAlO_2$ onto titanium dioxide allowed to overcome its low textural characteristics and increase surface basicity, providing therefore high catalytic activity (conversion of alcohol 94%, 24 h) and recyclability in carboxymethylation of allyl alcohol with DMC.[17] Application of low-cost slag-based materials prepared by the treatment of industrial desulfurization slag using various chemical agents and ultrasonication resulted in variable conversion of cinnamyl alcohol (8–85%) at similar selectivity towards the desired carbonate ester (ca. 80%).[18,19]

[a] Dr. N. D. Shcherban
L.V. Pysarzhevsky Institute of Physical Chemistry
NAS of Ukraine
31 pr. Nauky, 03028 Kyiv (Ukraine)
E-mail: nataliyalisenko@ukr.net

[b] Dr. N. D. Shcherban, E. Kholkina, Prof. D. Y. Murzin
Johan Gadolin Process Chemistry Centre
Åbo Akademi University
Henriksgatan 2, 20500 Turku/Åbo (Finland)
E-mail: dmurzin@abo.fi

[c] Dr. S. Sergiienko
Department of Inorganic Chemistry
University of Chemistry and Technology Prague
Technická 5, 16628 Prague 6 (Czech Republic)

[d] Dr. A. V. Kovalevsky
Department of Materials and Ceramics Engineering
University of Aveiro
3810-193 Aveiro (Portugal)

[e] Dr. I. Bezverkhyy
Laboratoire Interdisciplinaire Carnot de Bourgogne
UMR 6303 CNRS-Université de Bourgogne-Franche Comté
9 Av. A. Savary, 21078 Dijon Cedex (France)

Supporting information for this article is available on the WWW under https://doi.org/10.1002/cplu.202300600

Part of a joint Special Collection on the Applications of Porous Materials

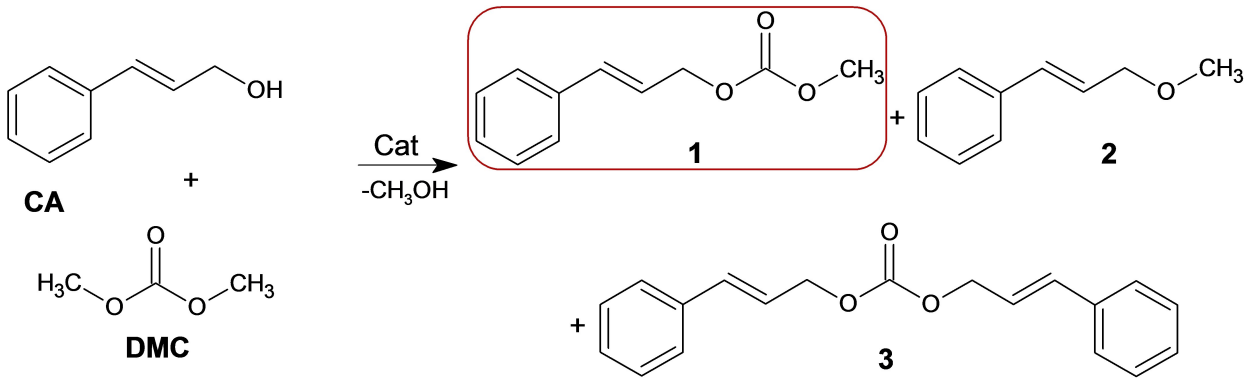

Scheme 1. Carboxymethylation of cinnamyl alcohol (CA) with dimethyl carbonate (DMC) yielding cinnamyl methyl carbonate (1) and side products – 1-phenyl-3-methoxy-1-propene (2) and dicinnamyl carbonate (3).

A theoretical study using DFT of 1-octanol carboxymethylation with DMC in the presence of $AlCl_3$ as a Lewis acid catalyst allowed to reveal a crucial role in proton-transfer processes of the dipole in Al–Cl covalent bonding.[20] Meanwhile, 99% yield of methyl octyl carbonate was reported over aluminium chloride (90 °C, 19 h).[20] Nanocrystalline ZSM-5 zeolite comprising of nanosized (20–30 nm) crystals was reported to catalyze carboxymethylation of alcohols more effectively compared to conventional zeolite (crystal size of 100–200 nm) due to a higher accessibility of the acid sites distributed over the developed surface facilitating diffusion of the reagents.[21] A sulfonated mesoporous polymer was found to be active giving almost complete conversion of primarily alcohols in carboxymethylation of a range of bio-derived alcohols into alkyl methyl carbonates. This result was associated with the developed mesoporosity and a high strength of the acid sites uniformly distributed over the catalyst surface.[22]

Graphitic carbon nitride, being a metal-free CN-material, has attracted a growing interest[24–32] in photocatalysis, electrocatalysis and traditional catalysis due to its polymeric and semiconductor nature as well as considering the worldwide concern of the society about global environmental issues. Promising catalytic activity and stability of graphitic carbon nitride in the Knoevenagel condensation of benzaldehyde with low-reactive ethylcyanoacetate and selective ethanol oxidation to acetaldehyde with molecular air has been reported in our previous papers.[33,34]

According to the authors knowledge, the data concerning the catalytic activity of graphitic carbon nitride in particular and metal-free basic materials in general in carboxymethylation of alcohols have not been reported in the open literature. A special attention in the current paper was given to the environmental-friendly synthesis of the above metal-free catalysts without using costly additional reagents and multistep synthetic procedures.

Therefore, the aim of the current study was to evaluate the catalytic performance of metal-free graphitic carbon nitride produced via a straightforward, green experimental protocol avoiding using templates and activating agents in carboxymethylation of cinnamyl alcohol chosen as a model lignin compound with DMC.

Results and Discussion

Characterization

XRD patterns (Figure 1a) of the prepared samples possess two main signals typical of graphitic carbon nitride. The most intensive peak at 2θ~27.3–27.4° indexed for graphite materials as (002) characterizes the interplanar distance in the layered aromatic system. The corresponding calculated interplanar distance of aromatic fragments *d* is 0.327–0.325 nm being slightly lower than for crystalline graphite (0.335 nm) and graphenes (0.353 nm).[35] A lower interplanar distance leading to a higher density between the layers for such aromatic systems containing heteroatoms can be associated with possible delocalization of electrons across the whole system, resulting in the increased interaction between the layers. The size of X-ray coherent-scattering region, determined by the broadening of the above signal at 2θ~27.3–27.4° using the Scherrer's equation, is ca. 10–12 nm. The second less intensive signal at 2θ~13.0–13.2° can be attributed to the structural packaging of carbon nitride in one layer. Some shifting of this peak to the higher 2θ values upon the transition from C_3N_4-2 to C_3N_4-8 should be noted. The lower calculated interplanar distance (0.681–0.671 nm) for the synthesized samples compared to the size of tri-*s*-triazine molecule (more than 0.73 nm) should be noted. Considering this interplanar distance corresponded to the size of one tri-*s*-triazine fragment, some slight distortion of the structure can be assumed.[36] Additionally, taking into account a smaller interplanar distance for C_3N_4-8 (0.671 nm) compared to C_3N_4-2 (0.681 nm), more distorted structure of C_3N_4-8 resulting obviously from the longer heat treatment of melamine can be concluded.

According to the data of CHN analysis (Table 1), the synthesized C_3N_4 samples along with nitrogen and carbon contain hydrogen (up to ca. 2 wt.%) which is associated with incomplete condensation of primary and secondary amino

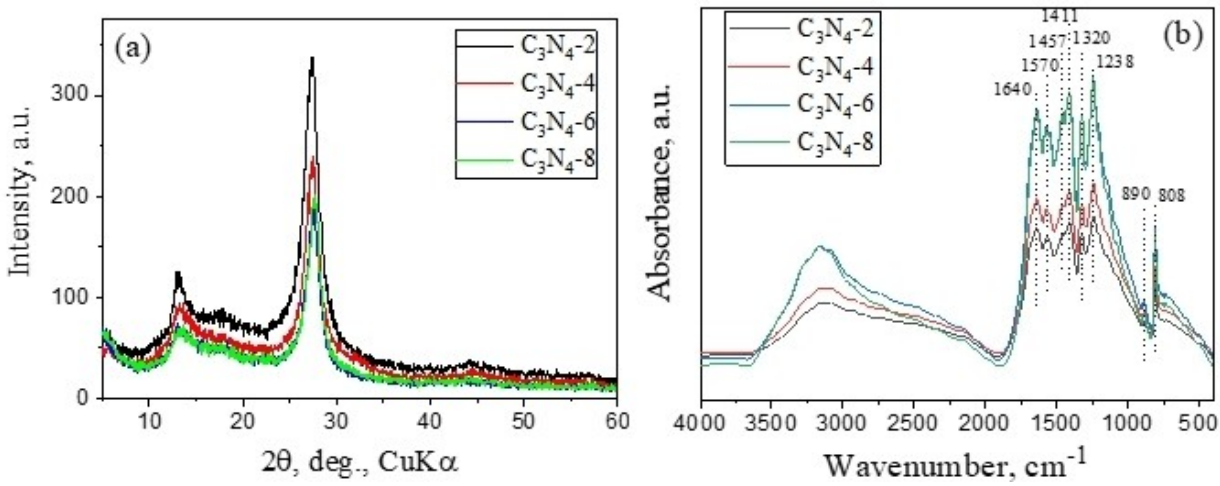

Figure 1. XRD patterns (a) and FTIR spectra (b) of the synthesized carbon nitride catalysts.

Table 1. Elemental composition of the synthesized carbon nitride samples.

Sample	Element content, wt.%				C/N atomic ratio
	C	N	H	Others	
C_3N_4-2	33.80	56.76	1.87	7.57	0.69
C_3N_4-4	34.29	59.37	1.82	4.52	0.68
C_3N_4-6	33.98	57.75	1.85	6.42	0.68
C_3N_4-8	33.49	54.67	1.98	9.86	0.71

groups located at the edges of graphene-like C–N sheets.[37] The atomic C/N ratios (0.68–0.71) being lower compared to the calculated value for ideal g-C_3N_4 (0.75) confirm the presence of amino group containing graphene-like C–N sheet edges.[38] A comparatively high content of other elements related obviously to oxygen should be noted (within the range of ca. 5–10 wt.%) which exceeds the oxygen content in similar materials described in other papers.[28,39] Along with CO_2, O_2 and moisture adsorbed on the sample surface from the atmosphere, oxygen can be also a part of various O-containing functional groups generated during the thermal treatment.[38] It is worth noting that the prolongation of the thermal treatment of melamine, namely heating exceeding 12 h, leads to its complete oxidation/combustion with formation of only combustion products.

FTIR spectra (Figure 1b) of the prepared materials contain the absorption band at around 810 cm^{-1} which is a characteristic feature of triazine/heptazine structures and caused by the bending vibrations of N–C=N bonds in these compounds[39–41] as well as a set of absorption bands in the range of 1238–1640 cm^{-1} originated from the stretching vibrations in heptazine cycles of graphitic carbon nitride.[42,43] The absorption band at ca. 890 cm^{-1} can be attributed to the deformation mode of N–H vibration.[44] The band centered at ca. 1411 cm^{-1} can be attributed to the C–N stretching vibration of the tertiary N atoms within the structure of carbon nitride, the peaks in the range of 1238–1320 cm^{-1} can be assigned to secondary bridging nitrogen atoms.[45] The band at 1640 cm^{-1} is due to the conjugated C–N stretching, the absorption bands in the range of 1457–1570 cm^{-1} correspond to the stretching vibration modes of the tri-s-triazine ring.[45] The broad absorption bands between 2900–3600 cm^{-1} correspond to the N–H and O–H stretching vibrations in uncondensed amino groups and hydroxyl groups/surface adsorbed water, respectively.[46]

The surface elemental composition and chemical state of the constituent elements of the prepared samples were determined using XPS (Figure 2). The most intense peak in C1s XPS spectra at binding energy of 287.9 eV (Figure 2a) corresponds to sp^2-bonded carbon in heptazine units (N–C=N coordination), while the signal centred at 284.6 eV originates from aromatic carbon atoms (sp^2 C–C bonds) confirming the presence of a carbon nitride phase.[47,48] The low-intense broad band centred at 293.6 eV is due to the excitation of plasmons in heptazine heterocycles.

N1s peak in the recorded XPS spectra can be approximated by a set of four components with maxima at binding energies of 398.5, 399.7, 400.9 and 404.3 eV (Figure 2b). The first signal can be attributed to sp^2-bonded N atoms in C–N=C fragments constituting heptazine heterocycles. The peak at ca. 399.7 eV is usually ascribed to nitrogen atoms coordinated with three carbon atoms (NC_3 species). The signal at ca. 400.9 eV corresponds to N atoms in the amino groups (–NH_2/–NH–) resulted from defective condensation of melon structures.[38] The broad signal with a maximum at ca. 404. eV can be due to the plasmon excitation of the aromatic heptazine system and/or quaternary nitrogen species.[44,49]

Calculated surface C/N atomic ratios being higher for the prepared samples (except for C_3N_4-8) than the corresponding expected value for stoichiometric carbon nitride (0.75) indicate the presence of excess carbon while longer heating of melamine (during 6–8 h) leads to a more complete condensation of the initial CN-precursor resulted in the formation of the materials with the C/N ratio close to the stoichiometric one.

The O1s signal centered at ca. 532 eV can be ascribed to the presence of hydroxyl groups and/or adsorbed water.[50]

Considering the obtained data on the general tendency of a decrease in both carbon and oxygen content as well as a

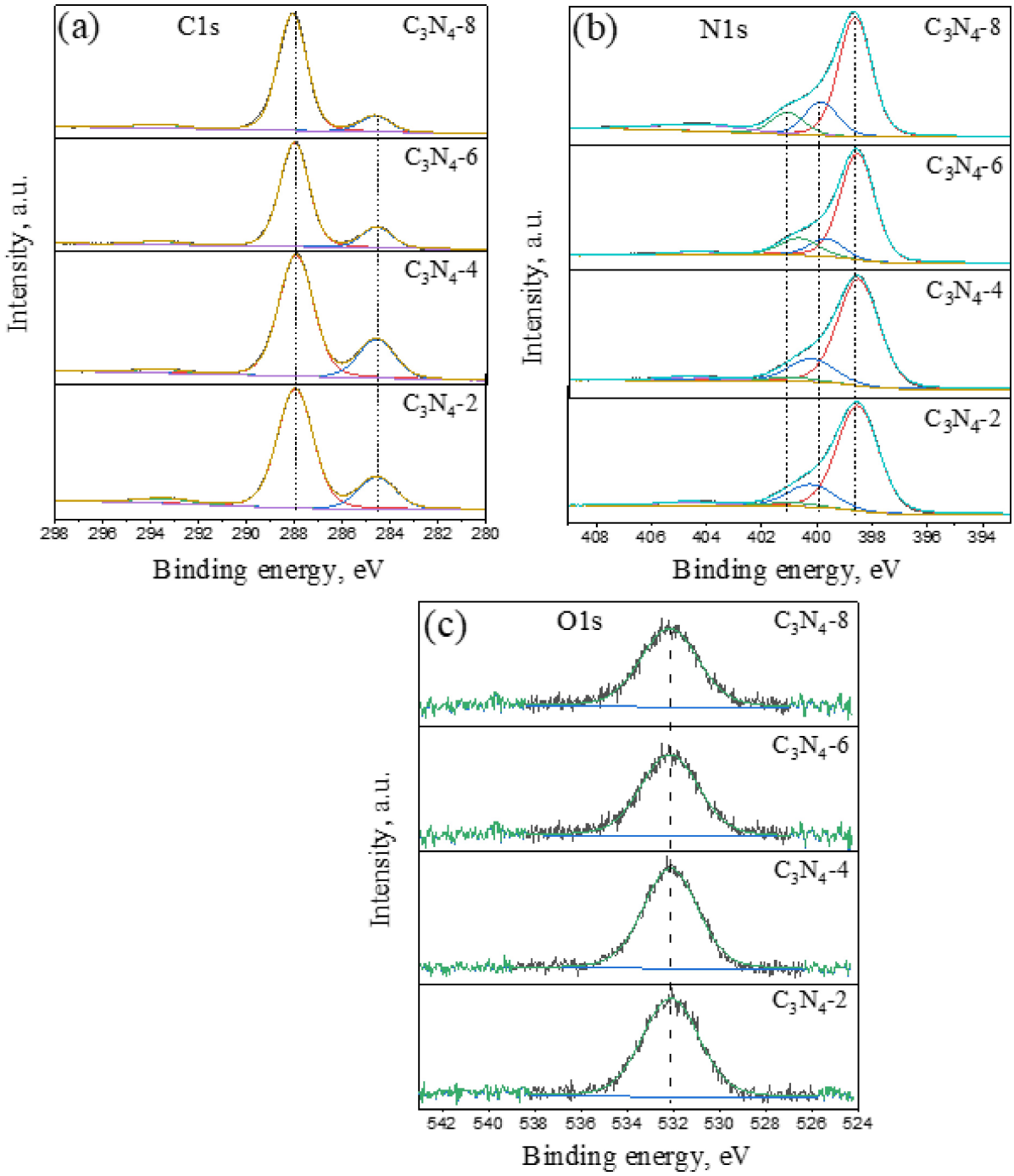

Figure 2. XPS spectra of C1s (a), N1s (b) and O1s (c) regions for the prepared samples.

resulting increase in nitrogen content (Table 2), certain amounts of carbon and oxygen are released obviously in the form of CO and CO_2 during longer thermal treatment of melamine.

According to the SEM measurements (Figure 3a–d), the prepared samples consist of microscopic formations mainly presented by lamellar particles and tubular structures which can be linked to the layered nature of graphitic carbon nitride. The tubular morphology of C_3N_4-8 is probably caused by the long-term heat treatment.

According to EDX mapping for the prepared carbon nitride samples (Figure 3e, f, Figure S1) a quite uniform distribution of the constituent chemical elements (C and N) as well as oxygen over the surface can be concluded.

Parameters of the porous structure of the synthesized graphitic carbon nitride samples were calculated from the isotherms of nitrogen adsorption-desorption (Figure 4) and listed in Table 3. The synthesized materials contain large mesopores (from 17 to 50 nm) as evidenced from the significant nitrogen adsorption at high relative pressures (p/p_0). The

Table 2. Surface composition of the obtained catalysts according to XPS data.

Sample	C1s			N1s				C/N ratio	O at. %
	C at. %	N–C=N	C=C	N at. %	C–N=C	NC_3	$–NH_2/–NH–$		
C_3N_4-2	44.8	74.7	20.5	53.3	75.4	18.0	3.1	0.84	1.9
C_3N_4-4	45.8	72.6	24.1	51.7	70.5	22.2	6.2	0.88	2.5
C_3N_4-6	43.1	79.6	16.4	55.6	72.7	12.0	13.1	0.78	1.3
C_3N_4-8	42.1	83.6	11.8	56.7	61.5	17.5	11.4	0.74	1.2

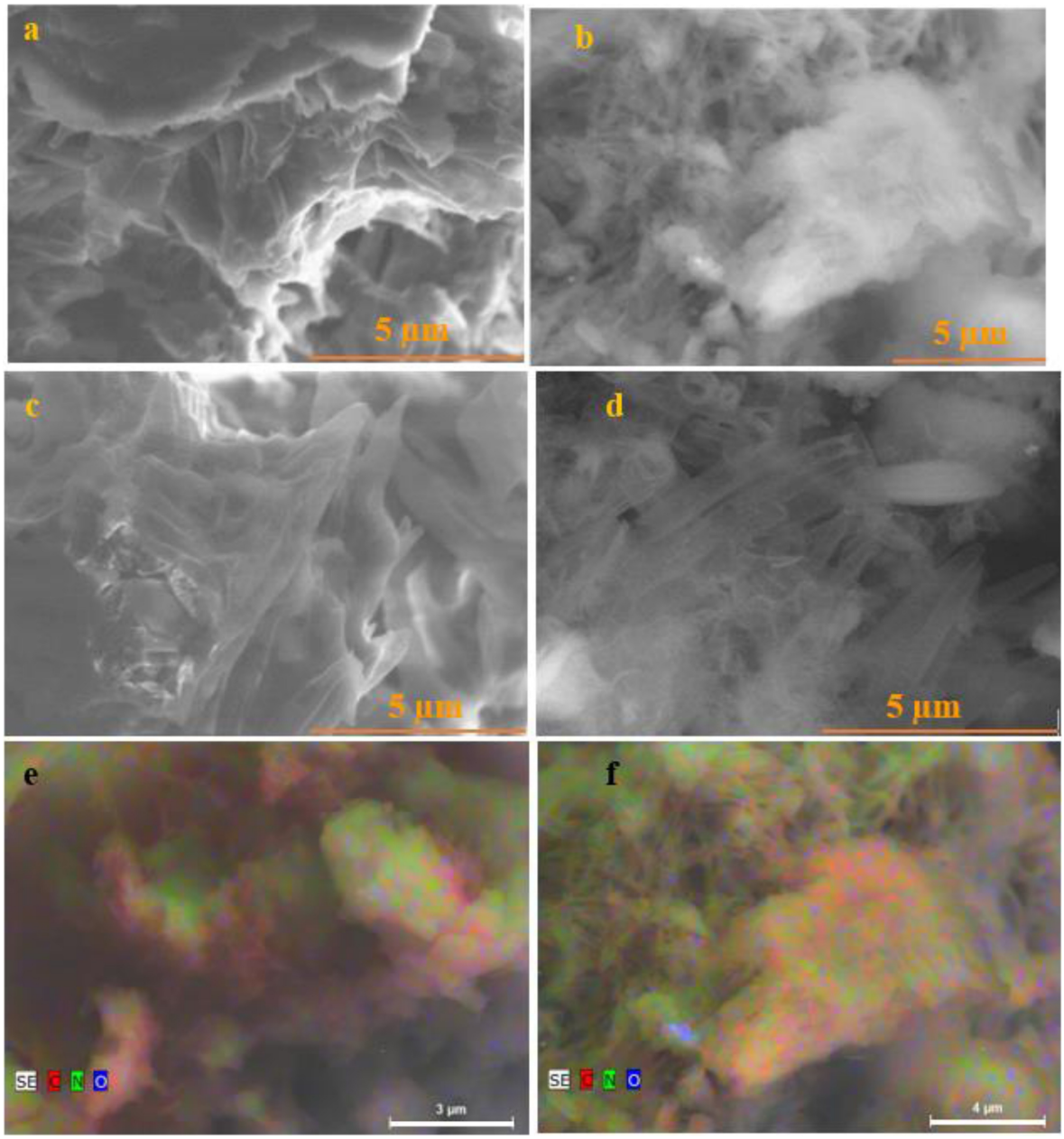

Figure 3. SEM images of C_3N_4-2 (a), C_3N_4-4 (b), C_3N_4-6 (c) and C_3N_4-8 (d); EDX maps of C_3N_4-2 (e) and C_3N_4-4 (f).

specific surface area and the total pore volume increased with the prolongation of melamine heat treatment namely from 10 m^2/g for C_3N_4-2 to 102 m^2/g for C_3N_4-8. Completely mesoporous structure except for C_3N_4-8 containing a very low micropore volume of 0.01 cm^3/g should be noted (Table 3). An increase in the specific surface area seems to be a reason for a higher oxygen content (according to CHN analysis) due to a

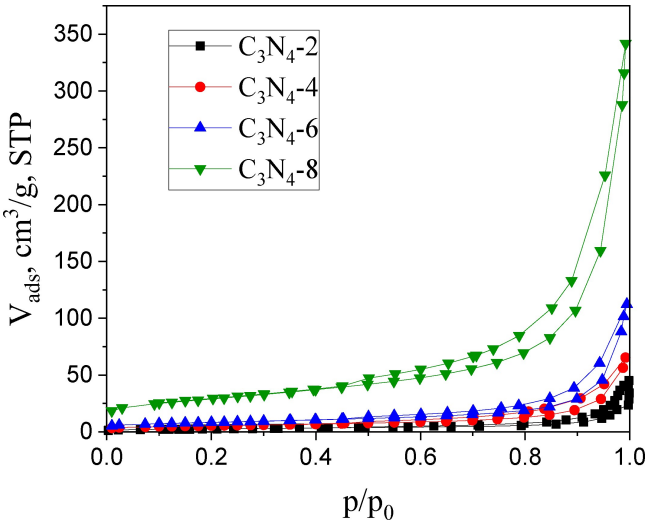

Figure 4. Nitrogen adsorption-desorption isotherms for the prepared carbon nitride. catalysts.

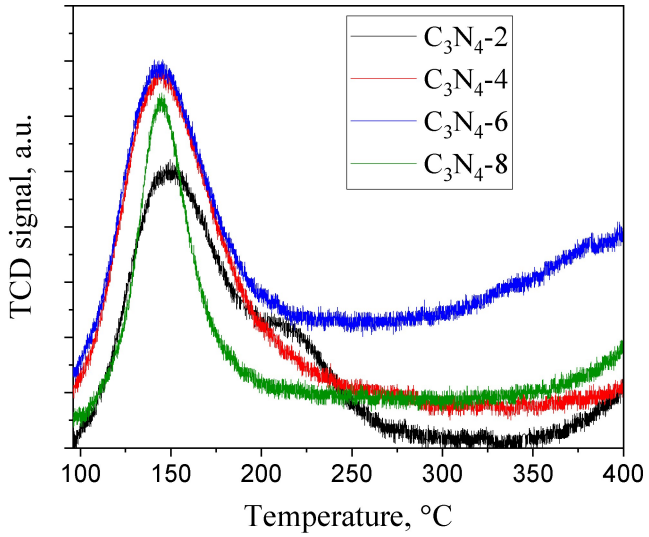

Figure 5. CO_2-TPD profiles for the synthesized carbon nitride catalysts.

Table 3. Parameters of the porous structure of the obtained materials (N_2, −196 °C).

Sample	V_{micro}, cm^3/g	V_{meso}, cm^3/g	D_{meso}, nm	S_{meso}, m^2/g	S_{BET}, m^2/g	V_{Σ}, cm^3/g
C_3N_4-2	0	0.06	~50	10	10	0.06
C_3N_4-4	0	0.10	~17	19	19	0.10
C_3N_4-6	0	0.17	~20	29	29	0.17
C_3N_4-8	0.01	0.52	~18	90	102	0.53

higher adsorption of O-containing gases (O_2 and CO_2) and moisture from the air.

The strength and concentration of basic sites of the obtained carbon nitride catalysts were evaluated using CO_2 temperature programmed desorption (CO_2 TPD). The corresponding curves contain one clear main desorption maximum at ca. 150 °C (Figure 5), which can be attributed to weak basic sites formed by nitrogen atoms in 6-membered triazine rings.[26] Based on the calculated concentration values of the basic sites, the studied materials can be arranged in the following order:

C_3N_4-4 (128) < C_3N_4-2 (147) < C_3N_4-6 (189) < C_3N_4-8 (219) μmol/g

In addition, weakly expressed shoulders centered at ca. 200 °C (Figure 5) and also ascribed to weak basic sites (maximum of CO_2 desorption below 250 °C) should be pointed out. The appearance of the CO_2 desorption at this temperature can be due to the presence of the NH species on the surface edges.[26]

Catalysis

The synthesized graphitic carbon nitrides were evaluated in carboxymethylation of cinnamyl alcohol with dimethyl carbonate (Table 4). Thermodynamic analysis provided in[19] confirmed some thermodynamic limitations in the synthesis of cinnamyl methyl carbonate and its subsequent reaction with CA being less prominent upon an increase in the temperature. More precisely such thermodynamic limitations suggest that complete conversion of CA to cinnamyl methyl carbonate cannot be reached being at the range of ca. 95%, which was confirmed by the experiments performed with triethylamine as the catalyst.[18] A blank experiment reported in the previous paper[19] showed ca. 10% of CA conversion after 24 h with selectivity towards the desired product of 69%.

The change of the conversion of cinnamyl alcohol with the reaction time (Figure 6a) demonstrates that the highest con-

Table 4. Carboxymethylation of cinnamyl alcohol with dimethyl carbonate over graphitic carbon nitrides.

Catalyst	Initial reaction rate (mmol/min g_{cat})	Conversion of cinnamyl alcohol after 24 h, %	Selectivity* to 1, %	Selectivity* to 2, %	Selectivity* to 3, %	Yield of 1 after 24 h, %
C_3N_4-2	0	57.2	90.4	1.77	0.71	52.4
C_3N_4-4	0.15	74.9	90.9	0.41	1.41	69.7
C_3N_4-6	0.17	90.0	95.5	0.23	1.19	81.7
C_3N_4-8	0.17	90.9	95.0	0.21	0.86	78.7

*Selectivity was determined at 50% conversion of cinnamyl alcohol.

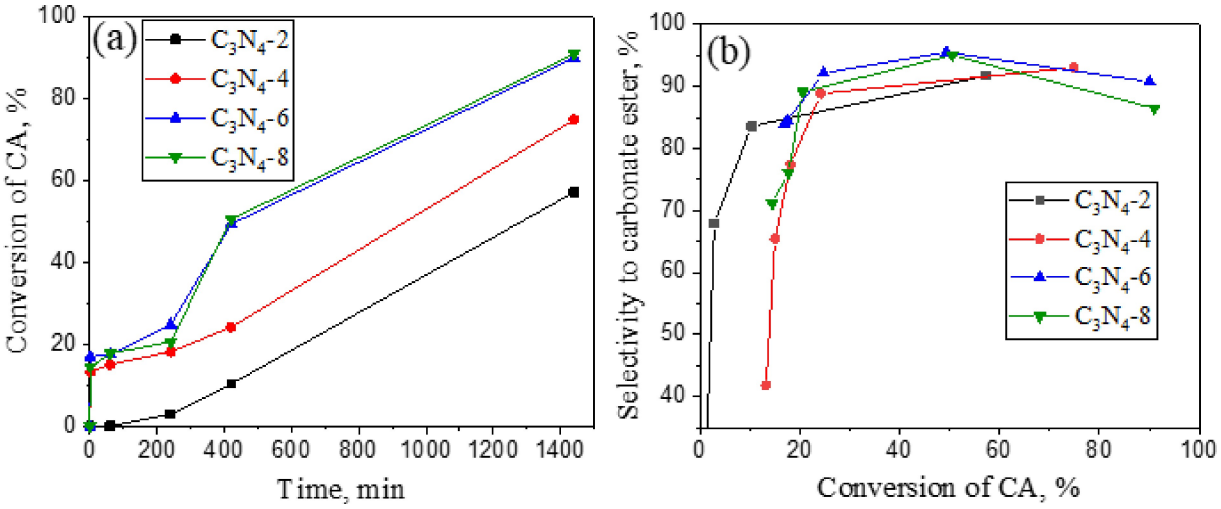

Figure 6. Conversion of cinnamyl alcohol (CA) as a function of the reaction time (a) and selectivity towards carbonate ester as a function of conversion (b) over the prepared graphitic carbon nitrides.

version of CA is reached over C_3N_4-6 and C_3N_4-8 (ca. 90–91 %). The highest transformation levels of the substrate over the above catalysts are associated with more developed porosity of these samples (Table 3) obviously originated from the more prolonged heat treatment of melamine. Inactivity of C_3N_4-2 at the beginning of the reaction and its further low activity during the first few hours (conversion ca. 3 % after 4 h) can be referred to the least developed and, as a result, the least accessible porous structure of this material.

As can be seen from the calculated initial reaction rates (Table 4) the reaction is characterized by similar rates over all studied samples except C_3N_4-2 (inactive at the beginning of the reaction).

Kinetic curves presented in Figure 6a exhibit either a gradual increase in conversion or even a sharp elevation after a certain time (ca. 200 min) similarly to the dependencies reported previously in.[19] Such an increase could be, in general, related to the apparent catalyst activation due to structural transformations, leaching of the catalytically active phase into the solution, removal of strongly adsorbed species of the reactants and products by methanol generated during the reaction as well as side transformations of CA and impurities presented in CA, such as hydrolysis of cinnamaldehyde to benzaldehyde. A reaction scheme featuring side products confirmed by NMR[19] is presented in Scheme 2. In addition to the reactions illustrated in Scheme 2 other side products outside of carboxymethylation pathway can be initially formed in a reversible step, blocking the surface sites. As the reaction proceeds, CA is transformed to carboxymethylation products pulling CA from the side products. In the latter case of the reaction graph with a so-called hanging vertex, initially a substantially amount of the side product should be formed and selectivity towards the desired product is expected to increase with conversion. Figure 6b depicting selectivity to the carbonate ester as a function of conversion clearly illustrates an increase of selectivity with conversion. A slight decrease in selectivity towards the carbonate ester in the presence of C_3N_4-6 and C_3N_4-8 beyond ca. 60 % conversion can be explained by the consecutive transformations of **1** to the product **3**. This is also visible from the dependency of the yield of product **3** vs

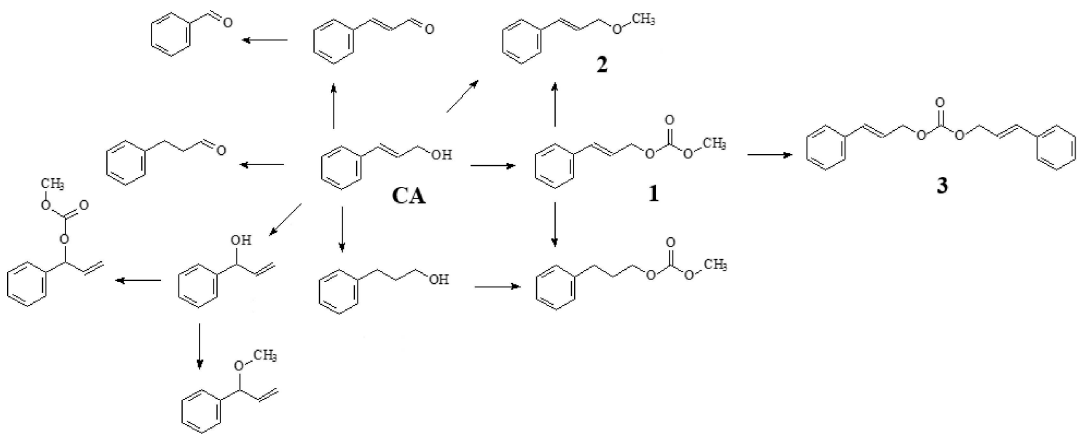

Scheme 2. Reaction network showing side products.

the yield of **1** presented in Figure S1, while the same figure illustrates almost parallel formation of **1** and **2.**

Figure 7 featuring the yields of different products as a function of times confirms that the yield of products other than the desired once is initially rather high especially for C_3N_4-4 gradually decreasing. Figure S2 presenting the yield of other products vs the yield of the desired product **1** shows a decline in the yield of the unwanted products with the consumption of the substrate. An increase in the final yield of other products over C_3N_4-6 (Figure S2d) is related to a change in the chemical composition of side products as selectivity to the unwanted products decreased substantially from ca. 58 to 4%.

The highest yield of the desired carbonate ester was obtained over C_3N_4-6 and C_3N_4-8 (ca. 82 and 79%, respectively). The highest catalytic activity of these samples can be related both to the more developed porosity and a higher concentration of basic sites determined by TPD CO_2 (190–220 μmol/g vs. 130–150 μmol/g for C_3N_4-2 and C_3N_4-4).

The highest catalytic activity expressed in TOF_t values (Figure 8a) is achieved over carbon nitride C_3N_4-4 considering similar initial reaction rates and the lowest basicity of this sample. C_3N_4-4 was also found to be the most active in terms of TOF_{24} value (Figure 8b) which can be connected with the lowest concentration of basic sites revealed by TPD CO_2 compared to other catalysts. The obtained TOF values significantly (by ca. 4 orders of magnitude) exceed the calculated results reported in the previous paper on slag-based catalysts,[18] which can be related to a much low concentration of basic sites in the catalysts studies herein.

Correlation of catalytic performance of the investigated carbon nitrides and their surface and structural characteristics is presented in Figure 9. As can be seen, selectivity toward the desired carbonate ester increases with the nitrogen atomic content determined from XPS (Figure 9a) reflecting thus the surface species rather than the overall N content and conversely decreases with an increase in the C/N atomic ratio (Figure 9b). As far as nitrogen species are concerned, a clear trend in an

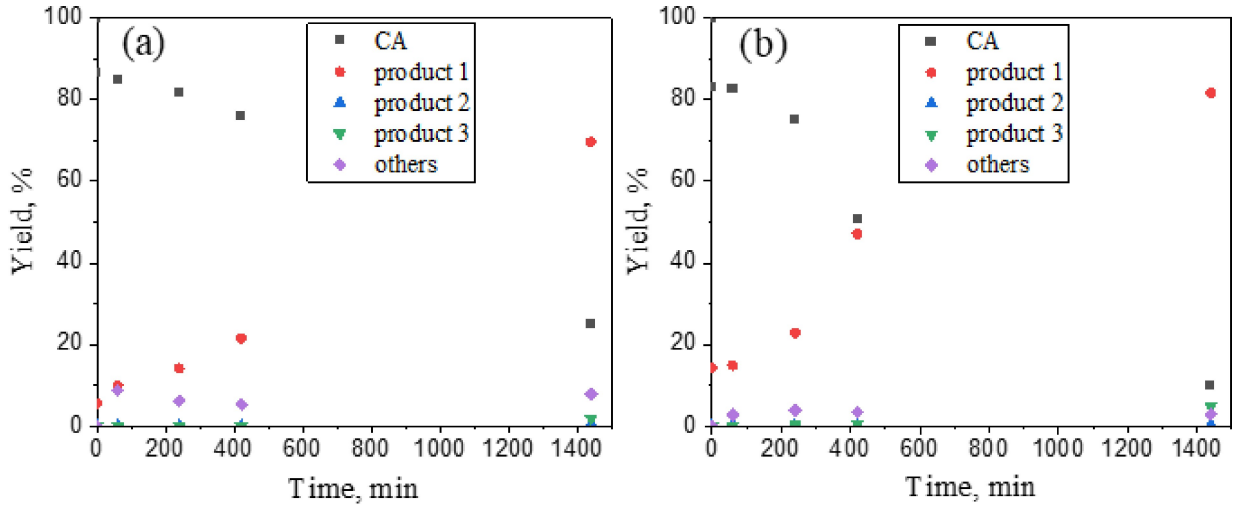

Figure 7. Concentration dependencies in CA carboxymethylation with DMC over C_3N_4-4 (a) and C_3N_4-6 (b).

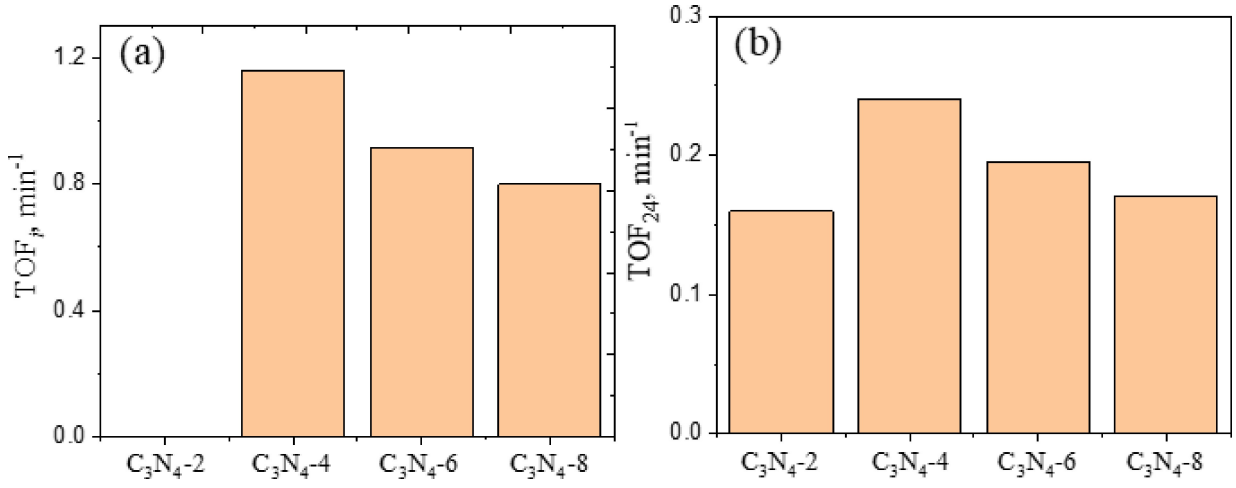

Figure 8. Carboxymethylation of CA with DMC over graphitic carbon nitrides: a) TOF_i and b) TOF_{24}. Calculations of TOF_i and TOF_{24} values correspond to 1 h and 24 h respectively.

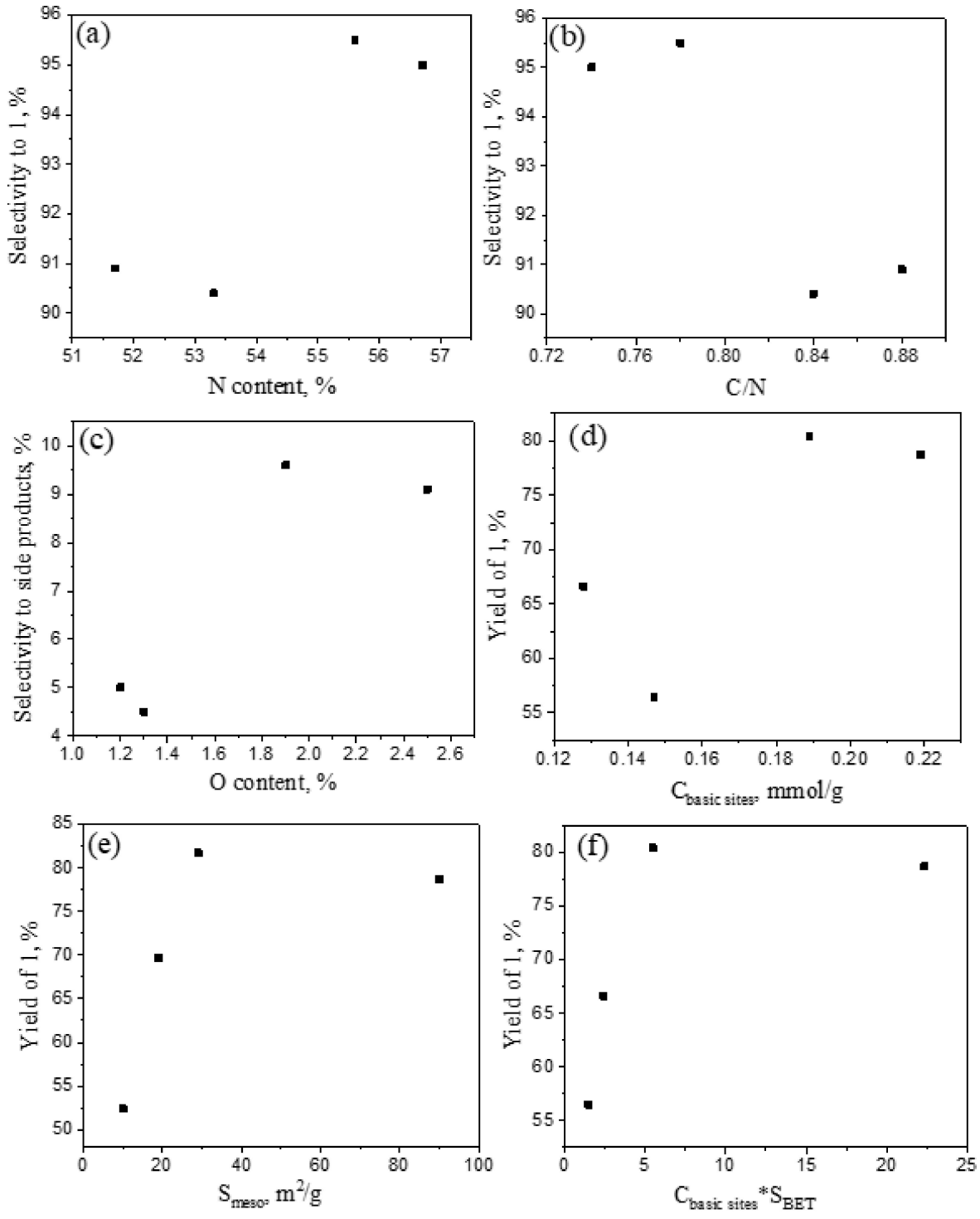

Figure 9. Selectivity (at 50% conversion of CA) towards carbonate ester as a function of a) N atomic content, b) C/N atomic ratio, c) selectivity towards the side products as a function of O atomic content (c) and d) yield of carbonate ester (after 24 h) as a function of the concentration of basic sites (d), mesopore specific surface area (e) and the parameter $C_{basic\ sites}$*S_{BET} (f) of the prepared carbon nitrides.

increase of the selectivity to the desired product with an elevation of the content of amino groups can be highlighted (Figure S3). Noticeably, selectivity towards side products increases with the O atomic content (the data from XPS, Figure 9c) indicating that O-containing surface species are more preferable for side reactions rather than the desired carboxymethylation. A general trend of the desired product yield increase upon elevation of the basic sites concentration determined from CO_2 TPD can be deduced from Figure 9d. Comparison of the catalytic data with the textural characteristics of the obtained metal-free catalysts (namely mesopore specific surface area) allowed to assume a favorable influence of

generated mesoporosity on the catalytic performance of the tested materials (Figure 9e). Similarly, the yield of the desired reaction product increases with an increase in the parameter $C_{basic\ sites}$*S_{BET} combining the influence of the concentration of basic sites ($C_{basic\ sites}$) and the surface area exposed to the reactants (Figure 9f).

The most active carbon nitride C_3N_4-6 catalyst was regenerated by washing with acetone followed by drying overnight in air at 100 °C and reused. According to the results of the recycling experiments (Figure 10a), the catalyst retained the initial activity not only in terms of CA conversion, but also selectivity towards the desired carbonate ester (95.3% at 50% conversion of CA). Such stable catalyst performance in terms of activity and selectivity after the catalyst recycling indicate absence of leaching of either N species or uncondensed nitrogen-containing fragments during the catalytic reaction. The unchanged XRD pattern of the spent catalyst (Figure 10b) testify that both the phase composition and the particle size of the catalyst remain the same providing an additional evidence of the catalyst stability. The obtained results testify the principle possibility of recycling and reusability of such metal-free catalysts being in line with our previous investigation of graphitic carbon nitride in gas-phase ethanol oxidation[30] where the excellent catalyst stability was demonstrated.

Generally, acid/base catalyzed carboxymethylation of alcohols with dimethyl carbonate proceeds through the transesterification mechanism.[20,22] The formation of an alkoxide ion apparently in the form of an N-alcoholate intermediate from the initial cinnamyl alcohol via its activation over N-containing base species located on the catalyst surface can be suggested as the first step (Figure 11). The subsequent nucleophilic attack of the carbon atom in DMC from the generated alkoxide ion results in an intermediate consisting of an ester and an alcohol connected with a carbon atom through an oxygen atom. Such an intermediate being unstable undergoes rearrangement with the formation of a new ester molecule (product **1**). Formation of the main side products (in particular, **3**) can proceed via a further interaction of the formed desired ester **1** with CA, being, however, rather limited (Table 4) due to the excess of DMC compared to the product **1**. It should be noted a more prominent generation of **3** over C_3N_4-4 possessing the highest surface O atomic content (Table 2). The side product 2 can be generated via the interaction of CA with methanol (a by-product of carboxymethylation) rather than decarboxylation of

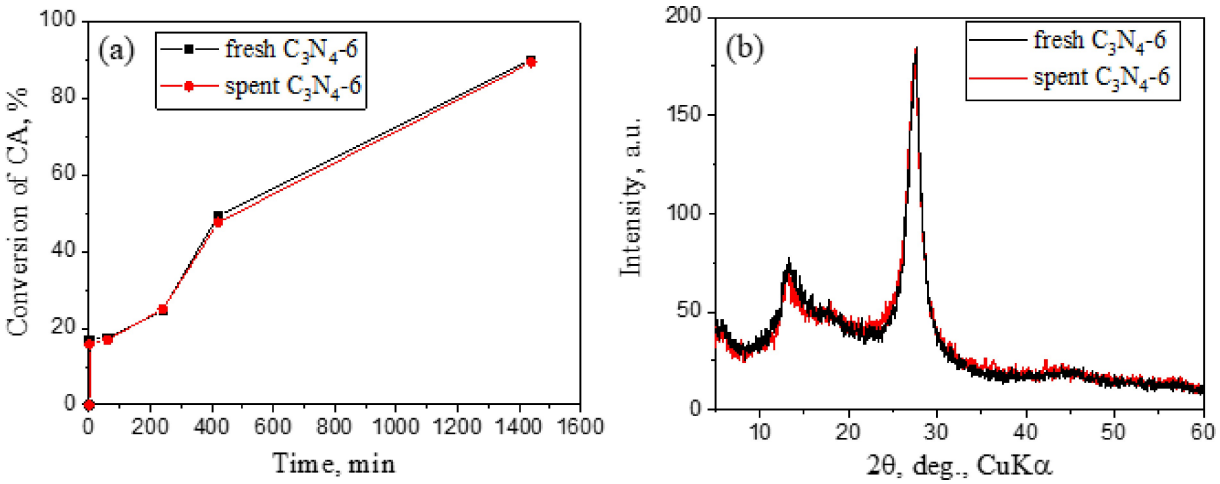

Figure 10. Dependence of CA conversion on the reaction time (a) and XRD patterns (b) for fresh and spent C_3N_4-6 catalysts.

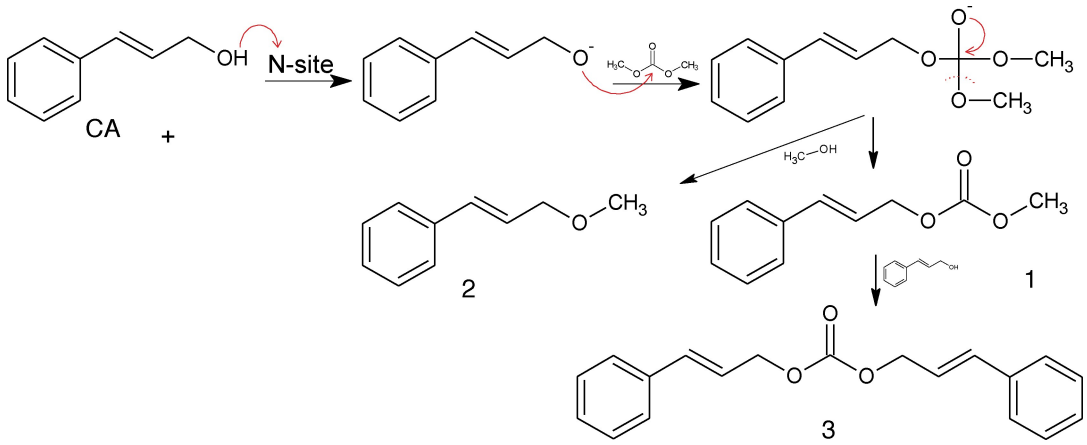

Figure 11. A plausible mechanism of carboxymethylation of cinnamyl alcohols with dimethyl carbonate over graphitic carbon nitride.

Table 5. Comparative data on the catalytic performance of various catalysts in carboxymethylation of alcohols.

Catalyst	Alcohol, concentration, mol/l	Alcohol/cat., wt./wt.	T, °C	Reaction time, h	Yield, %	Productivity, mol/h kg_{cat}	Ref.
K_2CO_3	Cinnamyl alcohol, 0.06	0.33	165	3	80.4	0.67	[16]
$CsF/\alpha Al_2O_3$	Cinnamyl alcohol, 0.06	0.33	90	50	76.1	0.04	[16]
NaX	Cinnamyl alcohol, 0.06	0.33	165	3	24.6	0.2	[16]
$NaAlO_2$	Cinnamyl alcohol, 1.19	3.35	90	8	96.0	3.0	[11]
Slag-based	Cinnamyl alcohol, 0.59	6.7	150	24	66.8	1.4	[18, 19]
$AlCl_3$	1-Octanol, 0.3	97.7	90	19	99.0	39.2	[20]
NZSM-5	1-Octanol, 0.5	0.87	110	48	96.0	0.13	[21]
C_3N_4-6	Cinnamyl alcohol, 0.3	7.92	170	24	81.7	2.01	This paper

the main product 1 taking into account similar tendencies in the changes of selectivity towards these reaction products.

Comparison of the performance of several reported in the literature catalysts and the materials described in the current paper is presented in Table 5. Considering differences in the alcohol type, concentration, alcohol/catalyst ratio, reaction temperature and time, for the sake of comparison the higher yields of carbonate esters obtained using mainly cinnamyl alcohol were taken into consideration. As can be seen, graphitic carbon nitride applied as a catalyst in this work allows to achieve a high yield of the corresponding carbonate ester comparable to other reported catalytic systems. A lower catalyst amount and correspondingly a higher alcohol to catalyst ratio used in the current work should be pointed out. A significantly higher value for $AlCl_3$ is a consequence of its good solubility in organic solvents. Carboxymethylation of cinnamyl alcohol over g-C_3N_4 providing a comparable catalytic performance operates at a high alcohol concentration and the alcohol/catalyst mass ratio indicating high productivity of the synthesized materials.

Specifically, application of the prepared metal-free catalysts afforded a high productivity of the desired carbonate ester (ca. 2 mol/h kg_{cat}) exceeding the corresponding values for previously described heterogeneous catalysts (Table 5). The corresponding highest numbers achieved with $AlCl_3$ and $NaAlO_2$ catalysts are obviously connected with a homogeneous process ($AlCl_3$) or its contribution ($NaAlO_2$) due to complete or partial solubility of the corresponding compounds.

The results of the current work indicate that graphitic carbon nitride obtained via a simple thermal treatment of melamine demonstrates promising catalytic activity in the carboxymethylation of cinnamyl alcohol with DMC. It should be noted that the synthetic procedure proposed hereby for the catalyst preparation is straightforward, cost efficient and environmentally friendly due to avoidance of any templates as well as additional chemicals and treatments.

Conclusions

Carboxymethylation of cinnamyl alcohol with dimethyl carbonate over metal-free graphitic carbon nitride produced from melamine via a straightforward experimental protocol has been demonstrated. Application of carbon nitride allowed to achieve at 170 °C high conversion of cinnamyl alcohol (up to 90%) at high selectivity (up to 95% at 50% conversion and ca. 91% after 24 h) towards the desired cinnamyl methyl carbonate. The highest yield of the desired reaction product was obtained with the catalyst synthesized by the longest heat treatment of melamine, which can be ascribed to a significant increase in the textural characteristics as well as an increase in the surface N atomic content accompanied by a decrease in the surface C and O content. The applied metal-free carbon nitride catalysts provide a higher productivity of the desired carbonate ester (ca. 2 mol/h kg_{cat}) compared to previously described heterogeneous catalysts.

Experimental Section

Catalysts preparation

Graphitic carbon nitride, labelled as C_3N_4-x, was prepared based on the previously described experimental procedure[51,52] with further modifications by heating melamine in air at 525 °C for a certain time, where x in the sample name corresponds to the heating time in hours. Therefore, for the preparation of C_3N_4-2 melamine was heated for 2 h, C_3N_4-4 – 4 h, C_3N_4-6 – 6 h and C_3N_4-8 – 8 h.

Characterization

The phase composition of the prepared carbon nitrides was determined using Bruker D8 Advance diffractometer equipped with Cu K_α ($\lambda = 0.15406$ nm) X-ray source.

The elemental analysis was performed using NCHS-analyzer Thermo Electron Flash EA1112.

Diffuse reflectance infrared spectra (IR spectra) were registered in 400–4000 cm^{-1} frequency range on a Perkin Elmer Spectrum One spectrometer using a diffuse reflectance accessory at the room temperature.

XPS-analysis was performed using HaXPES PHI Quantes spectrometer with an Al K_α X-ray source operated at 15 kV and 50 W. The pass energy of the analyzer was 55 eV and the energy step 0.05 eV.

The catalyst morphology was analyzed using the field emission SEM FEI Quanta 200 FEG. Images were obtained at an accelerating voltage of 15–20 kV and a beam current of 0.65 nA. Prior to imaging, the samples were coated by a platinum film of 15 nm thickness using a sputtering method.

Investigation of the porous structure of the synthesized materials was performed by nitrogen adsorption at −196 °C using Micromeritics 3Flex, after outgassing the samples at 150 °C under vacuum for 4 h. The specific surface area (S_{BET}) was calculated using the BET equation.[53] Mesopore size was determined by the Barrett-Joyner-Hallenda method from the desorption branch of the isotherm.[54] The isotherms were measured three times in order to obtain reproducible data.

Basic characteristics of the prepared catalysts were studied by temperature programmed desorption of carbon dioxide (TPD CO_2) using a Micromeritics Autochem 2910 equipment. Before the adsorption of CO_2, the sample was heated up to 200 °C (ramping rate 10 °C/min) in helium flow (10 ml/min) and kept at this temperature for 60 min. Afterwards, the investigated sample was cooled down to an ambient temperature and carbon dioxide was adsorbed to the catalyst for 30 min using a 50 ml/min flow. After the adsorption, the sample was flushed with helium (20 ml/min) for 30 min for the removal of physisorbed CO_2. The temperature programmed desorption was performed with a 10 °C/min heating rate up to 600 °C with the TCD signal registered every second.

Catalytic experiments

Carboxymethylation of cinnamyl alcohol (CA, Aldrich, 98%) with dimethyl carbonate (DMC, ReagentPlus®, 99%) applied both as a reactant and a solvent was performed in a 300 mL batch reactor (Parr Instruments) equipped with a mechanical agitator and a sampling line (with a 5 μm filter). The reactor was provided by an electrical heater and a water-cooling system. In a typical experiment, 0.5 g of the catalyst preheated at 110 °C overnight for the removal of moisture was applied. Cinnamyl alcohol (3.96 g) dissolved in 100 mL of the solvent as well as the dried catalyst were added into the reactor followed by its sealing and flushing with argon (AGA, 99.999%) for 10 min to remove air from the reaction media. Then the autoclave was pressurized up to 10 bar with argon and kept for 5 min for the leakage test. The temperature was increased to 170 °C (5 °C/min) and the final total pressure was elevated to 16 bar. The stirring speed of 540 rpm was applied to supress external mass transfer limitations. The stirring of the reaction mixture was started after reaching the desired temperature. The samples were periodically withdrawn from the reactor (10 s, 1 h, 4 h, 8 h and 24 h) and analysed by GC equipped with a DB-1 column (30 m, 250 μm, 0.50 μm). The peaks were identified via GC-MS (Agilent Technologies 5973 GC/MSD) equipped with a DB-1 column (30 m, 250 μm, 0.50 μm) and compared with the corresponding data for the reference compounds.

The conversion (X) of cinnamyl alcohol (CA), selectivity (S_i) and the product yields (Y_i) were calculated using the following equations:

$$X(\%) = \frac{c(CA)_0 - c(CA)_t}{c(CA)_0} \cdot 100 \quad (1)$$

$$S_i(\%) = \frac{c_i(product)_t}{\sum c_i(product)_t} \cdot 100 \quad (2)$$

$$Y_i(\%) = \frac{X \cdot S_i}{100} \quad (3)$$

Where $c(CA)_0$ and $c(CA)_t$ are the concentrations (mol/l) of CA in the reaction mixture initially and after a certain reaction time; $c_i(product)_t$ is the concentration (mol/l) of the specific reaction product i at time t.

The concentrations of the initial reagent and reaction products were determined using the corresponding response factors in GC analysis determined from the multipoint calibration curves.

The initial reaction rates were calculated for the first 60 min of the reaction according to eq. 4:

$$r_0(\text{mmol}/(\text{min}^*g_{cat})) = \frac{n(CA)_0 - n(CA)_{60\ min}}{60 \cdot m_{cat}} \quad (4)$$

where $n(CA)_0$ and $n(CA)_{60min}$ are the amounts (mmol) of CA in the reaction mixture initially and after 60 min; m_{cat} is the catalyst weight (g).

The initial turnover frequency calculated as the number of converted CA moles per moles of active sites per unit time was determined using the concentration of basic sites for the first 60 minutes of the reaction:

$$TOF_i(\text{min}^{-1}) = \frac{n(CA)_0 - n(CA)_{60\ min}}{t \cdot n_{(\text{basic sites})}} \quad (5)$$

where $n_{(\text{basic sites})}$ is the amount (mmol) of basic sites in the catalyst, as determined by CO_2 TPD and t – time (60 min).

The average turnover frequency (the total number of converted CA moles over basic sites after 24 h per unit time) was calculated according to eq. 6:

$$TOF_{24} = \frac{n(CA)_0 - n(CA)_{24\ h}}{t' \cdot n_{(\text{basic sites})}} \quad (6)$$

where t' – time (24 h).

The average catalyst productivity in 24 h ('CP' or the amount of the desired product formed per 1 kg of the catalyst in 1 h) was evaluated according to:

$$CP = \frac{n(CA)_0 \cdot Y_1}{100 \cdot t \cdot m_{cat}} \quad (7)$$

where Y_1 – the product yield after 24 h, t – time (24 h).

Supporting Information

Electronic Supplementary Information (ESI) available.

Acknowledgements

N. S. acknowledges the support of the National Research Foundation of Ukraine to the project "New effective zeolite catalysts for environmentally friendly processes of the conversion of renewable raw materials into valuable organic compounds" (project number 2020.02/0335) and the Verkhovna Rada of Ukraine to a personal scholarship for young scientists – doctors of sciences for 2021. The research was also supported by the Johannes Amos Comenius Programme, European Structural and Investment Funds, project 'CHEMFELLS V' (No. CZ.02.01.01/00/22_010/0003004). A. K. acknowledges the support of the project CICECO – Aveiro Institute of Materials

(UIDB/50011/2020, UIDP/50011/2020 & LA/P/0006/2020) financed by national funds through the FCT/MCTES (PIDDAC).

Conflict of Interests

The authors declare no conflict of interest.

Data Availability Statement

The data that support the findings of this study are available from the corresponding author upon reasonable request.

Keywords: carbonate esters · graphitic carbon nitride · carboxymethylation · heterogeneous catalysis · metal-free catalysts

[1] C. Martín, G. Fiorani, A. W. Kleij, *ACS Catal.* **2015**, *5*, 1353.
[2] J. Fournier, O. Lozano, C. Menozzi, S. Arseniyadis, J. Cossy, *Angew. Chem. Int. Ed.* **2013**, *52*, 1257.
[3] Q. Cheng, H. F. Tu, C. Zheng, J. P. Qu, G. Helmchen, S. L. You, *Chem. Rev.* **2019**, *119*, 1855.
[4] Y. Lee, S. Shabbir, S. Lee, H. Ahn, H. Rhee, *Green Chem.* **2015**, *17*, 3579.
[5] A. Serra-Muns, R. Pleixats, *J. Organomet. Chem.* **2010**, *695*, 1231.
[6] B. M. Trost, M. L. Crawley, *Chem. Rev.* **2003**, *103*, 2921.
[7] M. Chen, J. F. Hartwig, *J. Am. Chem. Soc.* **2015**, *137*, 13972.
[8] B. Schaffner, F. Schaffner, S. P. Verevkin, A. Börner, *Chem. Rev.* **2010**, *110*, 4554.
[9] M. A. Pacheco, C. L. Marshall, *Energ. Fuego At.* **1997**, *11*, 2.
[10] V. H. Wallingford, A. H. Homeyer, D. M. Jones, *J. Am. Chem. Soc.* **1941**, *63*, 2056.
[11] S. Ramesh, K. Indukuri, O. Riant, D. P. Debecker, *Org. Process Res. Dev.* **2018**, *22*, 1846.
[12] G. Fiorani, A. Perosa, M. Selva, *Green Chem.* **2018**, *20*, 288.
[13] M. Selva, A. Perosa, D. Rodriguez-Padron, R. Luque, *ACS Sustainable Chem. Eng.* **2019**, *7*, 6471.
[14] S. H. Pyo, J. H. Park, T. S. Chang, R. Hatti-Kaul, *Curr. Opin. Green Sustain. Chem.* **2017**, *5*, 61–66.
[15] P. Tundo, A. Perosa, *Chem. Rec.* **2002**, *2*, 13–23.
[16] J. N. Stanley, M. Selva, A. F. Masters, T. Maschmeyer, A. Perosa, *Green Chem.* **2013**, *15*, 3195.
[17] S. Ramesh, F. Devred, D. P. Debecker, *Appl. Catal. A* **2019**, *581*, 31.
[18] E. Kholkina, N. Kumar, K. Eränen, M. Peurla, H. Palonen, J. Salonen, J. Lehtonen, D. Y. Murzin, *Ultrason. Sonochem.* **2021**, *73*, 105503.
[19] E. Kholkina, N. Kumar, K. Eränen, V. Russo, J. Rahkila, M. Peurla, J. Wärnå, J. Lehtonen, D. Y. Murzin, *React. Kinet. Mech. Catal.* **2021**, *133*, 601.
[20] S. Jin, Y. Tian, C. R. McElroy, D. Wang, J. H. Clark, A. J. Hunt, *Catal. Sci. Technol.* **2017**, *7*, 4859–4865.
[21] D. Chevella, A. K. Macharla, R. Banothu, K. S. Gajula, V. Amrutham, M. Boosa, N. Nama, *Green Chem.* **2019**, *21*, 2938.
[22] K. S. Kanakikodi, S. R. Churipard, A. B. Halgeri, S. P. Maradur, *Sci. Rep.* **2020**, *10*, 1.
[23] H. Mutlu, J. Ruiz, S. C. Solleder, M. A. R. Meier, *Green Chem.* **2012**, *14*, 1728.
[24] A. Thomas, A. Fischer, F. Goettmann, M. Antonietti, J. O. Müller, R. Schlögl, J. M. Carlsson, *J. Mater. Chem.* **2008**, *18*, 4893.
[25] X. Wang, S. Blechert, M. Antonietti, *ACS Catal.* **2012**, *2*, 1596.
[26] J. Zhu, P. Xiao, H. Li, S. A. Carabineiro, *ACS Appl. Mater. Interfaces* **2014**, *6*, 16449.
[27] W. J. Ong, L. L. Tan, Y. H. Ng, S. T. Yong, S. P. Chai, *Chem. Rev.* **2016**, *116*, 7159.
[28] Q. Hao, G. Jia, W. Wei, A. Vinu, Y. Wang, H. Arandiyan, B. J. Ni, *Nano Res.* **2020**, *13*, 18.
[29] K. Srinivasu, B. Modak, S. K. Ghosh, *J. Phys. Chem. C* **2014**, *118*, 26479.
[30] P. Roy, A. Pramanik, P. Sarkar, *J. Phys. Chem. Lett.* **2021**, *12*, 2788.
[31] P. Roy, A. Pramanik, P. Sarkar, *J. Phys. Chem. Lett.* **2021**, *12*, 10837.
[32] K. Kumari, P. Choudhary, D. Sharma, V. Krishnan, *Ind. Eng. Chem. Res.* **2022**, *62*, 158.
[33] N. D. Shcherban, P. Mäki-Arvela, A. Aho, S. A. Sergiienko, P. S. Yaremov, K. Eränen, D. Yu. Murzin, *Catal. Sci. Technol.* **2018**, *8*, 2928.
[34] N. D. Shcherban, O. A. Diyuk, V. A. Zazhigalov, D. Yu. Murzin, *ACS Sustainable Chem. Eng.* **2021**, *9*, 5128.
[35] W. Ruland, B. Smarsly, *J. Appl. Crystallogr.* **2002**, *35*, 624.
[36] A. E. Raevskaya, Y. V. Panasiuk, G. V. Korzhak, O. L. Stroyuk, S. Y. Kuchmiy, V. M. Dzhagan, D. R. Zahn, *Catal. Today* **2017**, *284*, 229.
[37] Y. Zhao, Z. Liu, W. Chu, L. Song, Z. Zhang, D. Yu, Y. Tian, S. Xie, L. Sun, *Adv. Mater.* **2008**, *20*, 1777.
[38] L. Zhang, H. Wang, W. Shen, Z. Qin, J. Wang, W. Fan, *J. Catal.* **2016**, *344*, 293.
[39] J. Yu, S. Wang, B. Cheng, Z. Lin, F. Huang, *Catal. Sci. Technol.* **2013**, *3*, 1782.
[40] Z. Hong, B. Shen, Y. Chen, B. Lin, B. Gao, *J. Mater. Chem. A* **2013**, *1*, 11754.
[41] Y. Sui, J. Liu, Y. Zhang, X. Tian, W. Chen, *Nanoscale* **2013**, *5*, 9150.
[42] J. D. Hong, S. M. Yin, Y. X. Pan, J. Y. Han, T. H. Zhou, R. Xu, *Nanoscale* **2014**, *6*, 14984.
[43] J. Yu, K. Wang, W. Xiao, B. Cheng, *Phys. Chem. Chem. Phys.* **2014**, *16*, 11492.
[44] Y. Yang, Y. Guo, F. Liu, X. Yuan, Y. Guo, S. Zhang, M. Huo, *Appl. Catal. B* **2013**, *142*, 828.
[45] R. C. Dante, P. Martín-Ramos, F. M. Sánchez-Arévalo, L. Huerta, M. Bizarro, L. M. Navas-Gracia, J. Martín-Gil, *J. Solid State Chem.* **2013**, *201*, 153.
[46] F. Dong, Z. W. Zhao, T. Xiong, Z. L. Ni, W. D. Zhang, Y. J. Sun, W. K. Ho, *ACS Appl. Mater. Interfaces* **2013**, *5*, 11392.
[47] B. Long, J. Lin, X. Wang, *J. Mater. Chem. A* **2014**, *2*, 2942.
[48] D. ark, K. Lakhi, K. Ramadass, M. Kim, S. Talapaneni, S. Joseph, U. Ravon, K. Bahily-Al, A. Vinu, *Chem. Eur. J.* **2017**, *23*, 10753.
[49] J. Xu, Y. Wang, J. K. Shang, Q. Jiang, Y. X. Li, *Catal. Sci. Technol.* **2016**, *6*, 4192.
[50] M. J. Lima, A. M. Silva, C. G. Silva, J. L. Faria, *J. Catal.* **2017**, *353*, 44.
[51] A. L. Stroyuk, Y. V. Panasiuk, A. E. Raevskaya, S. Y. Kuchmy, *Theor. Exp. Chem.* **2015**, *51*, 243.
[52] N. D. Shcherban, V. V. Shvalagin, G. V. Korzhak, P. S. Yaremov, M. A. Skoryk, S. A. Sergiienko, S. Y. Kuchmiy, *J. Mol. Struct.* **2022**, *1250*, 131741.
[53] S. G. Gregg, K. S. W. Sing, *Adsorption, Surface Area and Porosity*, Acad. Press, New York, **1982**.
[54] E. P. Barrett, L. G. Joyner, P. P. Halenda, *J. Am. Chem. Soc.* **1951**, *73*, 373.

Manuscript received: October 20, 2023
Revised manuscript received: November 22, 2023
Accepted manuscript online: November 23, 2023
Version of record online: ■■, ■■

RESEARCH ARTICLE

Graphitic carbon nitride catalyses carboxymethylation of cinnamyl alcohol with DMC. Surface N species contribute to the selectivity towards the desired carbonate. Carbon nitride is one of the most productive in the investigated reaction.

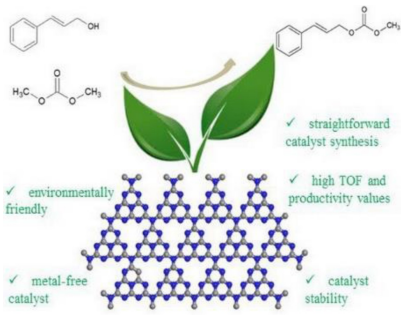

Dr. N. D. Shcherban, E. Kholkina, Dr. S. Sergiienko, Dr. A. V. Kovalevsky, Dr. I. Bezverkhyy, Prof. D. Y. Murzin**

1 – 14

Carboxymethylation of Cinnamyl Alcohol with Dimethyl Carbonate over Graphitic Carbon Nitrides